Heavy-ion irradiation effects on advanced perpendicular anisotropy spin-transfer torque magnetic tunnel junction

Odilia Coi, Gregory Di Pendina, Ricardo Sousa, Nomena Adrianjohany, David Dangla, Robert Ecoffet, Lionel Torres

Laser and Heavy Ion Irradiation Effects on Advanced Perpendicular Anisotropy Spin-Transfer Torque Magnetic Tunnel Junction

Odilia Coi, *Student Member, IEEE*, Gregory Di Pendina, Ricardo Sousa, Nomena Adrianjohany, David Dangla, Robert Ecoffet and Lionel Torres

***Abstract*—This paper investigates laser and heavy ion irradiation effects on Perpendicular Magnetic Anisotropy Spin Transfer Torque Magnetic Tunnel Junction devices (PMA STT-MTJ). The Radiative campaign will take place at the Université Catholique de Louvain (UCL) facility in April 2020. The considered devices consist of STT p-MTJs purely magnetic memories and they were fabricated using the most advanced CoFeB-MgO MTJ technology. Single-event upset (SEU) tolerance and modification of magnetic properties will be deeply investigated and presented in the final paper.**

I. Introduction

The Commercial Space dilemma afflicts designers of Space systems since they seek to ensure complex data processing, while obtaining, at the same time, a proper level of radiation tolerance, a reduced payload SWaP (Size, Weight and Power), and a competitive price.

Moreover, they are usually reluctant to use device without a significant space heritage that ensures a predictable behaviour. In an effort to create a solid harsh environment performances database for emerging devices, a considerable amount of research has been carried out in the exploration of technologies that aim to ensure a radiation tolerance higher than transistors in IC. Among them, Non-Volatile Magnetic Memories, already widely known for their nearly zero leakage performances and almost unlimited endurance [1], also show a very promising radiation hardness behaviour, due to their non charge based storage mechanism [2]. Starting from 2008, the qualification for space applications of these devices has been focused mainly on toggle MRAM due to the good maturity level of this technology at that time. This first generation of MRAM technology has been widely investigated. Honeywell [3] demonstrated the robustness of a 1 Mbit toggle MRAM up to a Linear Energy Transfer (LET) of about 78 MeV/mg/cm^2 and a cumulative fluence of 10^7 p/cm^2. Additionally, they reported negligible errors at higher LET [4]. Everspin memories evaluation also leads to heavy ion effects immunity conclusion [5]. However, the main drawback of toggle MRAM is the huge size, writing complexity and poor scalability [6]. For this reason, in the last few years, magnetic memory based on Spin Transfer-Torque (STT) switching mechanism gains the attention of the major semiconductor Companies. Comparative studies between Toggle-MRAM and STT-MRAM hybrid CMOS memory seem to suggest the latter to be more robust to heavy ion-induced hard error [7]. This could be explained by the smaller bit size and, more likely, by the different nano-pillar materials. Protons and gamma rays effect on in- plane STT magnetic stacks and devices are reported in [8]. Unfortunately, in-plane STT devices quickly showed their limits, so that the necessity to overcome them comes hand in hand with the need to improve reliability, power consumption and density by, respectively, improving the thermal stability, reducing the switching current, and eliminating the elliptical shape constraint. For these motivations, Perpendicular Anisotropy (PA) Co-Fe-B//MgO STT devices [9] represent today the most advanced and promising technology to achieve high density (over 1 Gb of memory capacity) application in harsh environment. To the best of our knowledge, only two previous studies explored the effect of radiations on STT-MRAM with PA. The first is a study on purely magnetic devices [10] where they found PA-Co-Fe-B to be insensitive to Single Event Upset (SEU) up to 15 MeV Si irradiation. The second [11] is a hybrid PA-STT/CMOS 55 nm memory device from Avalanche Technology: Total Ionizing Dose (TID) and heavy ion radiation response reporting optimistic results, even in presence of some unclear failure mechanism occurring in a small percentile of 350 cumulative test runs. The present work differs from the previous since it intends to be a preliminary study to the integration of these spintronic devices with the most advanced CMOS node. If the robustness to high LET is confirmed, one suitable strategy for future design could be to replace as many transistors as possible with magnetic devices, using the logic in memory concepts based on purely magnetic logic gate [12].

This work is organized mainly in two levels: in one hand, at stack level, it is focused on the radiation-induced effects on the atomic structure of a PA-STT film; on the other hand, at device level, to the Single Event Effect (SEE) on purely magnetic PA-STT memory arrays that are programmed by the use of an external board instead of peripheral CMOS circuit. Two kind of irradiation campaigns are planned with this aim: pulsed laser and heavy ion, in particular using $^{124}Xe^{35+}$ ions (LET in Si of 62.5 MeVcm^2/mg). During irradiation, the frame will be tilted to achieve various path lengths into the device. Since the interactions of heavy ions with matter create a plethora of unwanted effects such as target fragmentation, projectile fragmentations and neutrons, it is crucial to perform this preliminary study on purely magnetic memory array. Indeed, recoil atoms from MRAM stack's layers may be a threat for surrounding devices. For this reason, clear understandings on secondaries production could improve the IC design layout step, where the placement of transistors and spintronic device at different metal levels has to be done.

II. Devices under test

The Magnetic Tunnel Junction (MTJ) forms the basis for STT device fabrication and comprehension. As depicted in Fig. 1, this nano-pillar is composed of several layers of different materials, which could be mainly grouped as follows: a first Co/Fe/B (ferromagnetic alloy) layer, called Storage Layer, an insulating MgO tunnel barrier, a second Co/Fe/B layer called Reference Layer whose magnetization is pinned in a given direction. On its top, the so called Synthetic Antiferromagnetic Layer (SAF) is placed, where different layers of Co/Pt are alternated to increment the PA. A very thin layer of Ru is sandwiched between

them in order to guarantee the anti-ferromagnetic (AF) coupling. In contrast with toggle MRAM, STT- MRAM does not need an external magnetic field to be switched. Due to the property of Ferromagnetic (FM) materials, a charge flow through the MTJ leads to the generation of a spin-polarized current that, by exerting a spin-transfer torque on the magnetization, reverses the spin state. The direction of the current can be easily switched obtaining the mutual magnetization of the two Co/Fe/B layers to be parallel (logic value "0") or anti-parallel (logic value "1"). The magnetization state of the device can be sensed through the magneto-resistance phenomena, i.e. change in a material conductivity depending on the mutual magnetization state of the reference and storage layer.

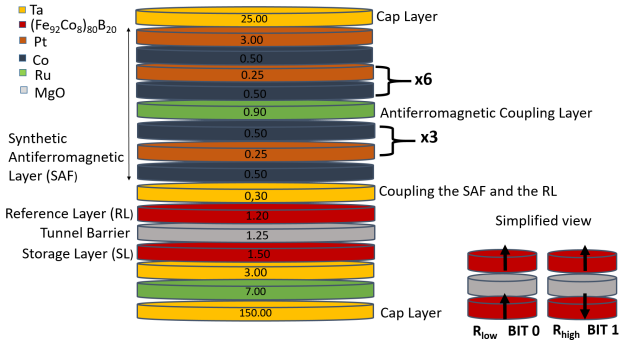

Fig. 1. Spin Transfer Torque Perpendicular Anisotropy Magnetic Tunnel Junction film stack. Numbers indicate the thickness of each layer in nm.

In this study, two groups of PA-STT devices are considered: the first consists of 4 memory matrix samples of PA-MTJ devices. They were fabricated by an Industrial Spintec's partner using the most advanced CoFeB-MgO technology and they are be investigated from the viewpoint of SEU tolerance. Each sample has a cross bridge structure of two metal wires for the top and bottom electrodes, which will be used to make four-terminal measurements. The fist group of PA-MTJ samples have different sizes resulting in a difference in the main device parameters, as detailed in Table I. They were received as bare die at our Laboratory, then wire bonded and packaged in PGA 84. A PCB has been designed to support these memory samples and all the connectors compatible with both Laser and Heavy ions test environments. Additionally, the board was designed to host 3 circuits in order to maximize the number of circuits in the vacuum chamber. To program the MTJ arrays the pad corresponding to V_{STT+} and V_{STT-} will be properly driven, trough the PCB, by the use of digital test board DPIN96 of the D10 Diamond Test Machine at SPINTEC. By the application of a voltage pulse of 0.6 V for a mean time of 50 ns all devices will be programmed in the anti-parallel state. Since the energy to flip the value from "1" to "0" is lower than the one needed to flip the bit in the opposite direction, we ensure, with this choice, to be in the worst case, i.e. the one easier to be switched leading to an SEU occurrence. This latter is simply detected by reading the memory state, letting a current of around 15 mA flows through the devices and thus sensing their resistance.

The second group of devices is intended to be investigated from the structural modification point of view by means of Transmission Electron Microscopy (TEM) before and after irradiation. Samples preparation is quite long, and is ongoing using CEA-LETI machines. (Fig. 2 (a)) . These films are based on SPINTEC stack and fabricated by SINGULUS Technology. The PA-MTJ nano-pillar typical parameters are highlighted in Table I. The expected TEM observable radiation's effects are:

TABLE I
MAGNETO-ELECTRICAL PARAMETERS OF THE DIFFERENT INVESTIGATED SAMPLES

Parameter	Symbol	First group Value range	Second group Value range
Critical Diameter [nm]	$\mathcal{CD}$	50-200	200
Tunnel Magnetoresistance	$\mathcal{TMR}$	50-150	100
Barrier Thickness [nm]	$\mathcal{T}_{ox}$	0.8-1	1.2-1.3
Resistance area Product [$\Omega\mu m^2$]	$\mathcal{RA}$	4	6

- Structural modifications at the interface AF-FM and FM-Insulator that could lead to MTJ parameters drift and switching voltage modifications
- Structural modification of the barrier with or without Oxygen depletion that lead to TMR reduction

Since the PA-MTJ is made of different material layers, it is interesting to investigate the energy and charge loss profile of the irradiation particles inside the insulating barrier and the ferromagnetic alloy since it shows a very high resistivity. For this aim, we use the TRADCARE Simulator as described in the next section.

III. TRADCARE SIMULATIONS

TRADCARE is an engineering tool developed by TRAD [13] and CNES. A multi-physics SEE prediction chain, Geant 4 Monte Carlo simulator, was developed and implemented in the TRADCARE software. In this work, TRADCARE has been used to analyse the interaction of heavy ions with PA-MTJ material layers in particular the MgO and the CoFeB alloy. The aim is to extract the LET profile, and the list of secondary products under the same conditions than UCL heavy ion test. To this purpose, a device model was created based on the density, resistivity and thickness of all the PA-STT MTJ atomic layers and the SPINTEC .gds file. Fig. 2 (b) shows the generated model in the simulation environment. It is important to underline the presence of metal layers (Cu, 300 nm) and via (W, 300 nm). In this first simulation, the MTJ is irradiated starting from the bottom layer, the closest to the MgO barrier, with a fluence of $8{\cdot}10^{12}$ ions/cm^2. Fig. 3 shows the LET profile across the complete stack. It has

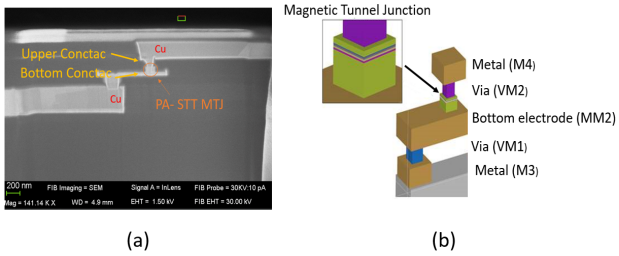

Fig. 2. Scanning electron microscope (SEM) image of a SPINTEC PA-STT MTJ (a).The corresponding PA-STT MTJ model created in the TRADCARE simulation environment (b).

been calculated using transport subroutine ICRU exported by g4em calculator. It is indicative at this point because straggling was not taken into account. It is interesting to note the large variation of LET values in the different layers of the structure. We noticed a maximum LET of 53 MeVcm^2/mg deposited in the MTJ. Further simulations are needed to confirm this value. One could of course question the validity of the notion of LET across such small dimensions. One could also question the validity of applying the classical Radiation Hardness Assurance (RHA)

approach of LET threshold criteria (in Si) to such multi-material nano-structures. This is clear if compared with Fig. 4 where LET and range of $^{124}Xe^{35+}$ in the different MTJ materials are depicted. Since the deposition of charge in the MgO layer is the

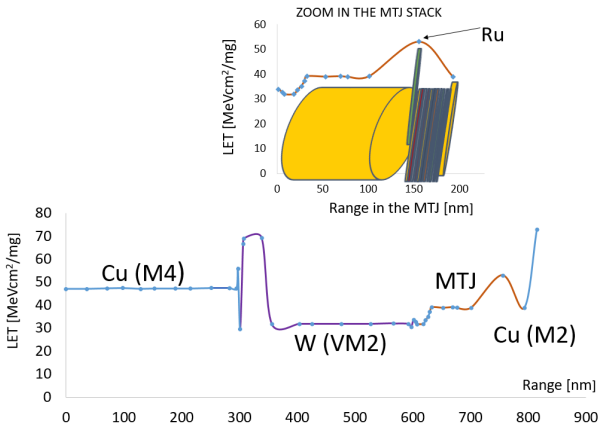

Fig. 3. $^{124}Xe^{35+}$ deposited LET across the complete stack: Metal 4 (Cu), Via (W), MTJ film and Metal 2 (Cu)

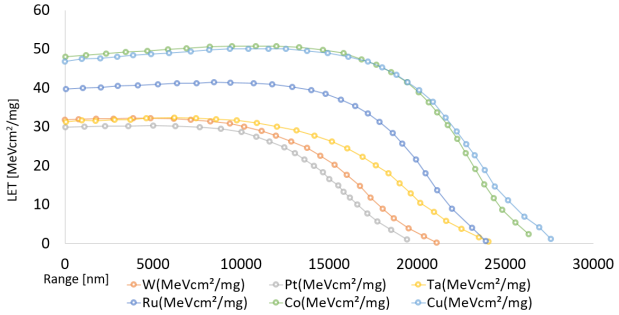

Fig. 4. LET of $^{124}Xe^{35+}$ in the different MTJ materials

most critical point for MTJ, among all the secondary products, we listed the ones that crossed the insulating barrier as depicted in the histograms of Fig. 5. In the same figure, the pie chart shows the amount of charge deposited in the sensitive volume (MgO) by each secondary product. Encouraging enough, most of the particle (76%) deposited a charge equal or lower than 1 fC. Only 0.0096% of the secondaries deposited a charge of 20 fC, value ten orders of magnitude smaller than the ones able to induce an immediate dielectric breakdown. The latter is triggered for an electric field of 0.7 V/nm for the considered samples.

IV. Laser and Heavy ions tests

The first experimental radiation campaign will take place at the end of March at CNES, in Toulouse. The test facility provides a Nd-YAG infrared laser producing 1064 nm, 7.19 ps pulses. It has the capability to map the exact spatial localization of the SEE occurrence and the capability of mapping the sensitive areas of the chip on an optical image. The optical specifications are detailed in Table II. An electrical control optical switch (pulse picker) is used to extract single pulses from the fast pulses train so that pulse frequency can vary from single shot to 40 MHz.

The range of laser's surface deposited energy can vary from few pJ to a maximum of 1.5 nJ. We will plot the laser cross section as a function of the different energy per pulse. During the irradiation, the DUT will be connected to the Diamond

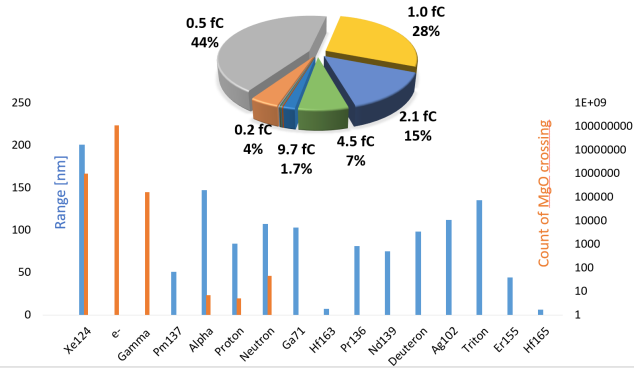

Fig. 5. List of the secondary products that crossed the MgO barrier. The crossing count is in logarithmic scale. The pie chart shows the distribution of the deposited charge in the sensitive volume.

TABLE II
Laser parameter

Parameter	Symbol	Value
Wave lenght [nm]	λ	1064
Pulse duration [ns]	τ	7.19
Spot size [μm]	d	1.1
Numerical aperture	$\mathcal{NA}$	0.71
Optical lens	$\mathcal{O.L.}$	x50

Test Machine. For each channel, a voltage driven resistance measurement will be done in order to detect any Single Event Transient (SET). Localized charges are generated in the DUT by single photon absorption. So far, we do not expect to have any SEU induced by thermal effect since, in PA-MTJ this kind of phenomena are triggered by energy in the order of μJ [14], a value much higher than the range used by the laser facility.

The second radiation experiment will be performed at the UCL Cyclotron (Université Catholique de Louvain), of Louvain-la-Neuve. For this experiment, the chosen ion species is the $^{124}Xe^{35+}$. The ion beam has a diameter of 25 mm and a homogeneity of 10%. The $^{124}Xe^{35+}$ beam is accelerated at an energy of 8 MeV/n, thus achieving a final kinetic energy of 995 MeV. Since our target is not Si we will not report classical LET data for this ion but, it has the highest LET value achievable at the facility. The cross section [cm^2/bit] will be calculated as:

$$\sigma = \frac{N_{\mathrm{SEU}}}{N_{\mathrm{bit}} \cdot \phi \cdot \cos(\theta)}$$

Where N_{SEU} is the total number of detected SEU events, N_{bit} is the total number of bits, ϕ is the ion fluence and θ is angle of incidence of the beam relative to the DUT [15]. Concerning the flux, we will start with a low flux of $5{\cdot}10^3$ ions/cm^2/s and then we will rise on to achieve a homogeneous strike probabilities over the DUT for a given LET and, to increase the probability of SEU occurrence. Actually, we expect to detect rare events, thus all the technical precautions, as for example the use of shielded cables and reduction of parasitic effects have been taken into account in the design of the experimental setup. The radiation effects will be inferred from the Current-Voltage characteristics measured in situ. Using Diamond Test Machine, a reference test condition program will be run periodically during the irradiation to check any degradation in device's parameters. Two kinds of measurements will be performed:

- **Real time dynamic measurement of the PA-STT MTJ resistance to detect both SET and SEU. This measurement will be done on the first device group.**
- **Static measurement, before and after the irradiation, on the totality of the SPINTEC samples to investigate the rise of structural modifications.**

V. Conclusion

A radiations effects study on advanced PA-STT is proposed. The simulated irradiation of the multi-layer structure with 995 MeV $^{124}Xe^{35+}$ ions indicates as non critical the deposited charge in the MgO sensitive volume, while suggesting a limit in the use of the traditional concepts of LET for such devices. The SEE sensitivity of these PA-STT MTJs will be addressed via additional experimental results, using both laser and heavy ions irradiation. The results will be provided in the final paper.

References

[1] H. Huai et al., Spin-transfer torque MRAM (STT-MRAM): Challenges and prospects, *AAPPS Bull*, vol.18, no 6, pp. 33-44, Dec. 2008.

[2] S. Gerardin et al., Present and Future non -volatile memories for space, *IEEE Trans. Nucl. Sci.*, vol.57, no 6, pp. 3016-3039, Aug. 2010.

[3] R. Katti et al., Heavy Ion and Total Ionizing Dose (TID) Performance of a 1 Mbit Magnetoresistive Random Access Memory (MRAM), *IEEE Radiation Effects Data Workshop*,Quebec City, QC, pp.103-105, 2009.

[4] R. Katti, Radiation-Induced Errors at Elevated Linear Energy Transfer Levels and Magnetic Error Rate Interactions in Magnetic Tunnel Junctions, *IEEE Radiation Effects Data Workshop*, San Antonio, TX, USA, pp.1-4, 2019.

[5] P. C. Adell, Single Event Effect Assessment of 1- Mbit Commercial Magneto-resistive Random Access Memory (MRAM), *IEEE Radiation Effects Data Workshop*, New Orleans, LA, USA, pp.1-4, 2017.

[6] B. Deny et al., Introduction to Magnetic Random Access Memory, *IEEE Press, WILEY* pp. 115-124, 2017.

[7] R. Katti et al., Heavy Ion Bit Response and Analysis of 256 Megabit Non-Volatile Spin-Torque-Transfer Magnetoresistive Random Access Memory, *IEEE Radiation Effects Data Workshop (REDW)*, pp. 1-4, 2019.

[8] H. Hughes, Radiations studies of spin-Transfer torque materials and devices, *IEEE trans. Nucl. Sci.*, vol. 59, no 6, pp. 3027-3033, Dec.2012.

[9] S. Ikeda, A perpendicular Anisotropy CoFeB-MgO Magnetic Tunnel Junction, *Nature Materials*, vol. 9, no 9, pp. 721-724, Sep. 2010.

[10] D. Kobayashi et al., Influence of Heavy Ion Irradiation on Perpendicular-Anisotropy CoFeB-MgO Magnetic Tunnel Junctions, *IEEE Trans. Nucl. Sci.*, vol. 61, no 4, pp. 1710-1716, August 2014.

[11] J. Ingalls, Total Dose and Heavy Ion Radiation Response of 55 nm Avalanche Technology Spin Transfer Torque MRAM, *Radiation Effects Data, IEEE Workshop*, 10.1109/REDW.2019.8906645, June 2019.

[12] D. Kobayashi et al., Chain of magnetic tunnel junctions as a spintronic memristor, *Journal of Appl. Physics* , 124, 152116;10.1063/1.5042431, 2018.

[13] N. Andianjohany et al., TRADCARE: Tool for SEE prediction in a radiation environment, presented at the ESA CNES Final Presentation, Mar.2017. [Online]. Available: https:// indico.esa.int/ event/ 188/ contributions/ 1662/ attachment/ 1523/ 1755/ TRADCARE_TOOL_for SEE_prediction_in_a_radiation_environment.pdf.

[14] M. Kharbouche-Herrari et al., Dual detection off Heating and Photocurrent attacks (DDHP) Sensor using Hybrid CMOS/STT-MRAM, *IEEE 25th International Symposium on On-Line Testing and Robust System Design (IOLTS)*, pp. 322-327, Sep. 2019.

[15] M. Bagatin and S. Gerardin, Ionizing radiation Effects in Electronics, *CRC Press, Taylor and Francis Group*, pp. 19-20, 2016.